Available online at www.sciencedirect.com
ScienceDirect
Ceramics International 38S (2012) S9–S12
CERAMICS INTERNATIONAL
www.elsevier.com/locate/ceramint

Effect of Sn:Ti variations on electric filed induced AFE–FE phase transition in PLZST antiferroelectric ceramics

Qiongna Zheng, Tongqing Yang *, Kun Wei, Jinfei Wang, Xi Yao

Functional Materials Research Laboratory, Tongji University, 1239 Siping Road, Shanghai 200092, China

Available online 30 April 2011

Abstract

The effect of Sn:Ti variations on antiferroelectric to ferroelectric phase transition of $(Pb_{0.97}La_{0.02})(Zr_{0.65}Sn_{0.35-x}Ti_x)O_3$ ($x = 0.08$–0.11) ceramics with compositions near antiferroelectric to ferroelectric morphotropic phase boundary was studied. X-ray diffraction showed that all samples were tetragonal phase at room temperature. With the increase of x from 0.08 to 0.1, all samples showed the typical antiferroelectric double loops. The critical value E_{AF} of the electric-field induced antiferroelectric to ferroelectric phase transition decreased from 64 kV/cm to 38 kV/cm, and the electric field E_{FA} of induced-ferroelectric to antiferroelectric phase transition decreased from 44 kV/cm to 10 kV/cm. A high polarization of the sample with $x = 0.1$ can be induced with a lower electric filed. The variations of Sn:Ti ratio had no effect on hysteresis of ΔE ($=E_{AF} - E_{FA}$), but ΔE reduced with temperature increasing. The virgin sample of which $x = 0.11$ was intrinsic antiferroelectric phase, but the remanent polarization of induced-ferroelectric phase remained after electric-field was removed at room temperature.

Keywords: A. Powders: solid state reaction; C. Ferroelectric properties; D. PZT; Antiferroelectric

1. Introduction

$PbZrO_3$ was the first reported antiferroelectrics which have a high phase transition electric-field of antiferroelectric (AFE) to ferroelectric (FE). Then, Ti^{4+}, Sn^{4+} and La^{3+} were modified into B site or A site of $PbZrO_3$ for lowering the phase transition electric-field, and lead lanthanum zirconate stannate titanate antiferroelectric system (PLZST) were developed [1–4]. PLZST tetragonal antiferroelectrics can be induced to rhombohedral ferroelectrics by an applied electric-field, accompanied with nonlinear increase of polarization and strain [5]. These materials can be applied in high-energy storage capacitors [6], explosive electrical transducers [7], actuators [8], pyroelectric detectors [9], antiferroelectric cold cathode materials [10], ferroelectric refrigeration [11], and so on. In these applications, materials with a lower external applied electric-field for antiferroelectric (AFE) to ferroelectric (FE) phase transition are desired. PLZST antiferroelectric materials are most attractive antiferroelectric materials these years, which have a wide adjusting range of AFE and FE phase by varying the compositions [12–14]. But most of the PLZST antiferroelectric materials still show a high phase transition electric-field which is difficult to induce AFE to FE phase transition. The materials with compositions near antiferroelectric and ferroelectric morphotropic phase boundary (MPB) have the small free energy difference between AFE and FE, and lower phase transition electric-field [1]. In this paper, the effect of Sn:Ti variations on electric filed induced AFE–FE phase transition in PLZST antiferroelectric ceramics near the MPB was studied for tailoring AFE–FE phase transition behaviors.

2. Experimental procedure

A series of compositions near MPB with varying Sn:Ti ratios were selected here, and their compositions were shown in Table 1. The starting materials used were Pb_3O_4, La_2O_3, ZrO_2, SnO_2 and TiO_2 according to the compositions of Table 1 with an addition of 1 wt.% excess Pb_3O_4. The samples were prepared by solid reaction synthesis. The raw materials were first mixed and pre-sintered at 900 °C for 2 h, then pressed to 10 mm diameter pellets and sintered at 1200 °C for 2 h. Phase analyses of the sintered samples were tested by X-ray diffraction (Model No. D8, manufactured by Bruker AXS, Germany). Some of the

* Corresponding author. Tel.: +86 21 65980544; fax: +86 21 65985179.
E-mail address: yangtongqing@tongji.edu.cn (T. Yang).

0272-8842/$36.00
doi:10.1016/j.ceramint.2011.04.037

Table 1
Compositions with varying Sn:Ti ratios of PLZST antiferroelectric ceramics.

Designation	Composition	Sn:Ti ratio
A1	$(Pb_{0.97}La_{0.02})(Zr_{0.65}\ Sn_{0.24}Ti_{0.11})O_3$	24:11
A2	$(Pb_{0.97}La_{0.02})(Zr_{0.65}\ Sn_{0.25}Ti_{0.10})O_3$	25:10
A3	$(Pb_{0.97}La_{0.02})(Zr_{0.65}\ Sn_{0.255}Ti_{0.095})O_3$	25.5:9.5
A4	$(Pb_{0.97}La_{0.02})(Zr_{0.65}\ Sn_{0.26}Ti_{0.09})O_3$	26:9
A5	$(Pb_{0.97}La_{0.02})(Zr_{0.65}\ Sn_{0.27}Ti_{0.08})O_3$	27:8

samples were then polished and covered with gold electrode for properties measurement. The polarization–electric field hysteresis loop (*P–E*) was measured using Radiant Precision Premier (Model No. II, manufactured by Radiant Technologies Inc., USA).

3. Results and discussion

X-ray diffraction patterns of virgin samples at room temperature are shown in Fig. 1. As shown, all the virgin samples (A1–A5) are tetragonal phase according to the existing of the characteristic peaks (0 0 2), (2 0 2), (1 0 3) of tetragonal phase, i.e., the samples of $(Pb_{0.97}La_{0.02})(Zr_{0.65}Sn_{0.35-x}Ti_x)O_3$ with $x = 0.08$–0.11 are antiferroelectrics.

Fig. 2 shows the polarization–electric field loops (*P–E* loops) of sample A2 under different applied electric-fields at room temperature. As shown, a classic double-hysteresis loop characteristic of AFE phase was observed, and the remnant polarization was zero after applied electric-field was removed. The meanings of E_{AF} and E_{FA} are also given in Fig. 2. E_{AF} is the critical value of the electric field induced AFE to FE phase transition, and E_{FA} is the critical value of the electric field at which induced-ferroelectric recovers to antiferroelectric phase. ΔE ($=E_{AF} - E_{FA}$) is the hysteresis of electric filed induced phase transition, it represents the thermal stability of FE phase induced by external applied electric field. Later, we will show that ΔE depends strongly on the temperature, which decrease linearly with the increasing of temperature. In application design of actuator, lower E_{AF} is desired for small applied electric field, and lower ΔE is desired for small nonlinearity. Large ΔE will lead to heating of materials and lever down the properties of devices, especially at high frequency.

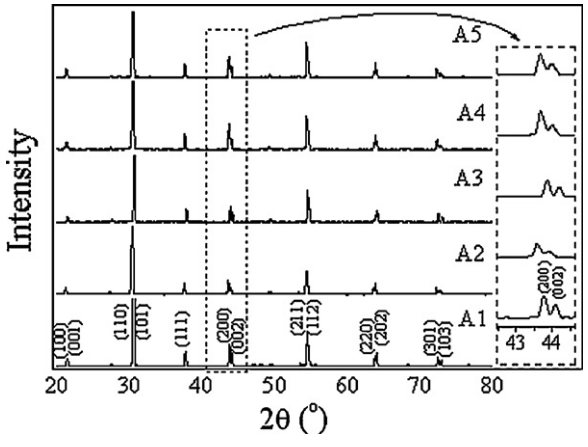

Fig. 1. XRD patterns of virgin samples at room temperature. Insert: enlargement of the dashed frame.

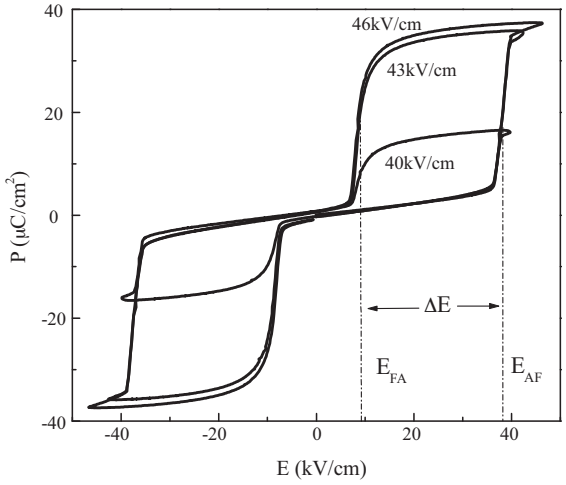

Fig. 2. The variation of polarization with different applied fields of sample A2.

The *P–E* loops of all the samples at room temperature are shown in Fig. 3. As shown in Fig. 3(a), the typical antiferroelectric double hysteresis loops are represented for A2, A3, A4

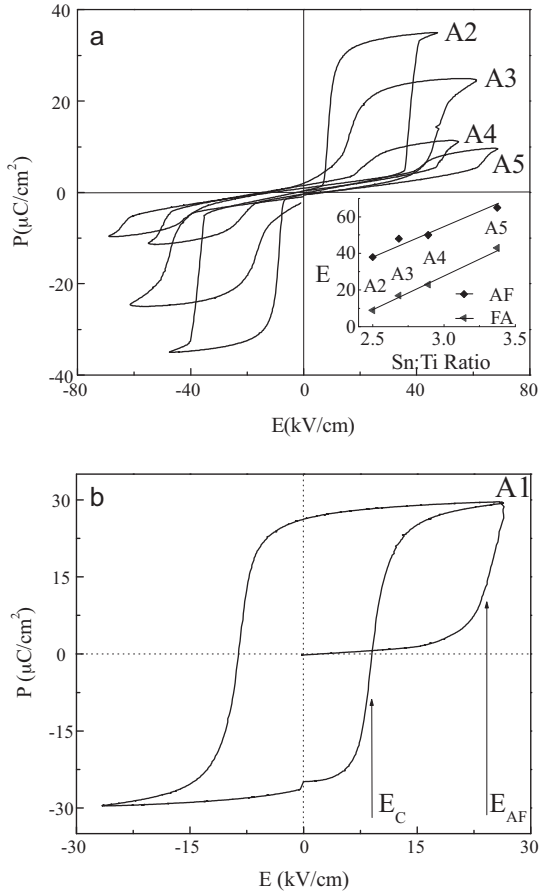

Fig. 3. *P–E* loops at room temperature. (a) A2–A5 compositions. Insert: variations of E_{AF} and E_{FA} with different Sn:Ti ratios; (b) virgin sample of A1 composition.

and A5, the critical values E_{AF} are 38, 46, 51 and 64 kV/cm, the critical values E_{FA} are 10, 19, 27 and 44 kV/cm, respectively. We noted the E_{AF} increased as Sn content increased. It is known that the composition moved further from the MPB with the Sn content increasing, AFE phase was more stable. As a result, it required a higher electric field of E_{AF} to induce more stable AFE phase to FE phase. For the induced FE phase, a high polarization of about 38 μC/cm^2 of sample A2 is observed.

We also noted that the polarization of the samples decreased with the increasing of its E_{AF}. From Fig. 2, the polarization increased rapidly when the applied electric-field was near E_{AF}, and saturated gradually when the applied field was higher than E_{AF}. In measurement, we found if the value of E_{AF} was too high, the samples were easy to be broken down by applied electric-field before the polarization reached the saturation state. As a result, it is difficult to obtain the *P–E* loops with saturated polarization for more stable AFE samples.

Fig. 3(b) shows the *P–E* loop with first cycle of virgin sample of A1 at room temperature. As shown, virgin sample was first induced from AFE to FE phase with a high induced field of E_{AF} = 2.4 kV/mm. Different from other samples, the polarization of A1 remained after applied electric-field was removed. Then, a classical *P–E* loop of FE phase with coercive field of E_C = 0.9 kV/mm was observed. Obviously, the critical field E_{AF} of AFE phase was larger than the coercive field E_C of FE phase, i.e., the virgin sample was intrinsic AFE phase for composition A1, which is coincident with XRD pattern shown in Fig. 1. The FE phase of composition A1 is induced by applied electric-field, which is unstable and easy to recover to AFE phase again at some conditions [15].

The temperature dependence of E_{AF} and E_{FA} for sample A2 is shown in Fig. 4. We noted that, with the increasing of temperature, the E_{AF} changed slightly, but the E_{FA} increased rapidly. It is known that the FE phase with high polarization is induced from AFE phase by applied electric field in Fig. 4, which is unstable, and easy to recover to AFE phase at E_{FA}. As a result, with the increasing of temperature, the induced FE phase recover to AFE phase at higher E_{FA}, i.e., the E_{FA} increased and the hysteresis ΔE (=$E_{AF} - E_{FA}$) decreased, as seen in Fig. 4. So, the value of ΔE represent the thermal stability of the induced FE phase, higher applied electric field is needed to stabilize the induced FE phase at higher temperature.

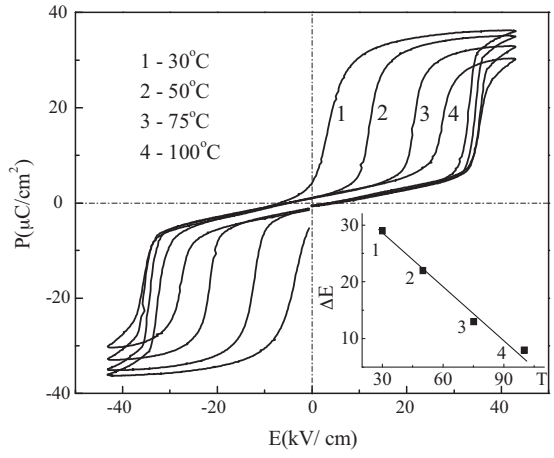

Fig. 4. Temperature dependence of E_{AF} and E_{FA} for sample A2. Insert: variations of ΔE with different temperatures.

As mentioning above, lower E_{AF} and lower ΔE are desired for the application of actuator. On the other hand, higher operating temperature is not suitable for applications. So, we also tried to tailor the phase transition properties by composition modification. Insert in Fig. 3(a) shows the variations of E_{AF} and E_{FA} with composition. As shown, the E_{AF} and E_{FA} are remarkably modified by the change of composition. With decreasing of Sn:Ti ratio, the lower E_{AF} was obtained, but the E_{FA} also decreased simultaneously. As a result, the hysteresis ΔE (=$E_{AF} - E_{FA}$) showed no significant change, that means the ΔE is difficult to be tailored by Sn:Ti ratio at present case. In our previous study and other reports [12,16], it was found that ΔE was related closely with Curie temperature T_c. Lower ΔE was obtained by decreasing T_c and modified with Ba addition in A site. Further study is still in progress.

4. Conclusion

The samples $(Pb_{0.97}La_{0.02})(Zr_{0.65}Sn_{0.35-x}Ti_x)O_3$ (x = 0.08–0.11) with compositions near AFE–FE morphotropic phase boundary were prepared. X-ray diffraction showed the virgin samples A1–A5 were all tetragonal phase at room temperature. With the increase of Sn:Ti ratio, the critical value E_{AF} of samples A2–A5 increased from 38 kV/cm to 64 kV/cm, and E_{FA} increased from 10 kV/cm to 44 kV/cm. Sn:Ti variations had no effect on the hysteresis ΔE of electric filed induced phase transition, but ΔE reduced with temperature increasing. Different from others samples, the ferroelectric phase of sample A1 induced by the applied electric field can remain after electric field was removed at room temperature, and the remanent polarization of ferroelectric phase was about 30 μC/cm^2.

Acknowledgements

This work is supported by the National Natural Science Foundation of China (No. 10874130), the Key Project of Chinese Ministry of Education (No. 108055), Shanghai Pujiang Program and the State Key Laboratory of Electronic Thin Films and Integrated Devices (UESTC).

References

[1] D. Berlincourt, Transducers using forced transitions between ferroelectric and antiferroelectric states, IEEE Transactions on Sonics and Ultrasonics 13 (1966) 116–125.
[2] W.Y. Pan, C.Q. Dam, Q.M. Zhang, L.E. Cross, Large displacement transducers based on electric field force phase transitions in the tetragonal $(Pb_{0.97}La_{0.02})(Ti,Zr,Sn)O_3$ family of ceramics, Journal of Applied Physics 66 (1989) 6014–6023.
[3] W. Chan, Z. Xu, Y. Zhang, T. Hung, H. Chen, Microstructural evolution and macroscopic property relationship in antiferroelectric lead lanthanum stannate zirconate titanate ceramics, Journal of Applied Physics 94 (2003) 4563–4565.
[4] X. Chen, H. Li, D. Li, F. Cao, X. Dong, Study on slim-loop ferroelectric ceramics for high-power pulse capacitors, Chinese Physics Society 57 (2008) 7298–7304.

[5] P. Liu, T.Q. Yang, Z. Xu, L. Zhang, X. Yao, Electric field induced antiferroelectric to ferroelectric phase transition of Pb(Zr, Sn, Ti)O_3 ceramics and tailoring of properties through composition modification, Acta Physics Sinica 49 (9) (2000) 1852–1858.
[6] A.Q. Jiang, T.A. Tang, S. Corkovic, Q. Zhang, Reversible charge injection in antiferroelectric thin films, Applied Physics Letters 93 (21) (2008) 212908.
[7] Y. Feng, Z. Xu, F. Chen, X. Yao, Antiferroelectric ceramic applied to explosive electrical transducers, Piezoelectrics and Acoustooptics 27 (2) (2005) 156–159.
[8] O. Essig, P. Wang, M. Hartweg, P. Janker, H. Nafe, F. Aldinger, Uniaxial stress and temperature dependence of field induced strains in antiferroelectric lead zirconate titanate stannat ceramics, Journal of the European Ceramic Society 19 (1999) 1223–1228.
[9] T.Q. Yang, P. Liu, Z. Xu, L. Zhang, X. Yao, Tunable pyroelectricity in La-modified PZST antiferroelectric ceramics, Ferroelectrics 230 (1999) 181–186.
[10] Z. Sheng, Y. Feng, Z. Xu, X. Sun, X. Huang, Experimental investigation of antiferroelectric cold cathode for strong electron emission, Journal of Xi'an Jiaotong University 42 (8) (2008) 977–981.
[11] P.D. Thacher, Electrocaloric effects in some ferroelectric and antiferroelectric Pb(Zr,Ti)O_3 compounds, Journal of Applied Physics 39 (1968) 1996–2002.
[12] K. Markowski, S.E. Park, S. Yoshikawa, L.E. Cross, Effect of compositional variations in the lead lanthanum zirconate stannate titanate system on electrical properties, Journal of the American Ceramic Society 79 (12) (1996) 3297–3304.
[13] L. Wang, Q. Li, L. Xue, X. Liang, Effect of Ti^{4+}:Sn^{4+} ratio on the phase transition and electric properties of PLZST antiferroelectric ceramics, Journal of Materials Science 42 (2007) 7397–7401.
[14] P. Liu, X. Yao, Dielectric properties and phase transitions of ($Pb_{0.87}La_{0.02}Ba_{0.1}$)($Zr_{0.6}Sn_{0.4-x}Ti_x$) O_3 ceramics with compositions near AFE/RFE phase boundary, Solid State Communications 132 (2004) 809–813.
[15] T.Q. Yang, X. Yao, Metastable ferroelectric phase in lanthanum-doped lead zirconate titanate stannate antiferroelectric ceramics, Ceramics International 34 (2008) 715–717.
[16] Q.N. Zheng, T.Q. Yang, Y.W. Luo, X. Yao, Effect of barium additions on dielectric properties and phase transitions in (Pb, La)(Zr, Sn, Ti)O_3 antiferroelectric ceramics, Ferroelectrics 403 (2010) 54–59.